MDPI

Article

Effect of Dielectric Thickness on Resistive Switching Polarity in TiN/Ti/HfO_2/Pt Stacks

Guillermo Vinuesa [1,*], Héctor García [1], Mireia B. González [2], Kristjan Kalam [3], Miguel Zabala [2], Aivar Tarre [3], Kaupo Kukli [3], Aile Tamm [3], Francesca Campabadal [2], Juan Jiménez [4], Helena Castán [1] and Salvador Dueñas [1]

[1] Department of Electronics, University of Valladolid, Paseo de Belén 15, 47011 Valladolid, Spain; hecgar@ele.uva.es (H.G.); helena@ele.uva.es (H.C.); sduenas@ele.uva.es (S.D.)
[2] Institute of Microelectronics of Barcelona, IMB-CNM (CSIC), Campus UAB, 08193 Bellaterra, Spain; mireia.bargallo.gonzalez@csic.es (M.B.G.); miguel.zabala@imb-cnm.csic.es (M.Z.); francesca.campabadal@imb-cnm.csic.es (F.C.)
[3] Institute of Physics, University of Tartu, W. Ostwaldi 1, 50411 Tartu, Estonia; kristjan.kalam@ut.ee (K.K.); aivar.tarre@ut.ee (A.T.); kaupo.kukli@ut.ee (K.K.); aile.tamm@ut.ee (A.T.)
[4] GdS Optronlab, Department of Condensed Matter Physics, LUCIA Building University of Valladolid, Paseo de Belén 19, 47011 Valladolid, Spain; jimenez@fmc.uva.es
* Correspondence: guillermo.vinuesa@alumnos.uva.es

Abstract: In recent years, several materials and metal-insulator-metal devices are being intensively studied as prospective non-volatile memories due to their resistive switching effect. In this work, thickness-dependent resistive switching polarity was observed in TiN/Ti/HfO_2/Pt structures as the sign of the voltages at which SET and RESET occur depended on the film thickness. A thorough revision of the previous literature on bipolar resistive switching polarity changes is made in order to condense previous knowledge of the subject in a brief and comprehensible way and explain the experimental measurements. The different resistive switching polarities occur in a similar voltage range, which is a new finding when compared to precedent research on the subject. A hypothesis is proposed to explain the change in resistive switching polarity, based on the assumption that polarity change is due to filament disruption occurring at different interfaces.

Keywords: resistive switching; thickness dependence; conductive filaments; RRAM; polarity change; hafnium oxide

Citation: Vinuesa, G.; García, H.; González, M.B.; Kalam, K.; Zabala, M.; Tarre, A.; Kukli, K.; Tamm, A.; Campabadal, F.; Jiménez, J.; et al. Effect of Dielectric Thickness on Resistive Switching Polarity in TiN/Ti/HfO_2/Pt Stacks. *Electronics* **2022**, *11*, 479. https://doi.org/10.3390/electronics11030479

Academic Editor: Jung-Hun Seo

Received: 18 January 2022
Accepted: 4 February 2022
Published: 6 February 2022

Publisher's Note: MDPI stays neutral with regard to jurisdictional claims in published maps and institutional affiliations.

Copyright: © 2022 by the authors. Licensee MDPI, Basel, Switzerland. This article is an open access article distributed under the terms and conditions of the Creative Commons Attribution (CC BY) license (https://creativecommons.org/licenses/by/4.0/).

1. Introduction

Non-volatile resistive random-access memories (RRAM) based on the resistive switching (RS) effect are of increasing interest due to their characteristics, such as small cell size and low operating voltages, as well as simple device structure composed of metal-insulator-metal (MIM) junctions. The RS effect occurs when conductive filaments (CF) grow in a dielectric film between two metal electrodes by applying an electric field. After these CFs are formed for the first time (electroforming process), certain voltage values can be applied to either break (RESET process) or form the CFs again (SET process) [1–5]. In the case of MIM devices where the dielectric is an oxide and none of the metal electrodes is electrochemically active, the filament is formed by oxygen vacancies (valence change mechanism or VCM), otherwise the filament would be formed by migration of metal cations (usually Ni, Ag or Cu) from the electrochemically active electrode (electrochemical metallization effect or ECM) [6]. When these voltage values are of a different sign, the phenomenon is called bipolar resistive switching (BRS) [5]. BRS can present different polarities, commonly referred to clockwise RS or CW (SET process at negative voltages and RESET process at positive voltages) and counter-clockwise RS or CCW (SET process at positive voltages and RESET process at negative voltages). The RS effect is depicted by a current–voltage (I-V) hysteretic curve, which presents two current values for each applied voltage value.

If the RRAM device degrades, this curve can become unstable (non-repeatable), leading to cycle-to-cycle variability, which is one of the main issues of current RRAM technology. However, it has been observed that some RS systems have the ability to be regenerated after being stressed by applying an appropriate voltage cycle [7].

In the context of resistive switching media, HfO_2 has been one of the most extensively studied dielectrics for the fabrication of RRAM [8–12] due to its relevant electrical properties. However, although the RS mechanism has been heavily studied and theorized about in general [13] and specifically for HfO_2 [14], the previously published literature on the switching polarities is scarce, which nonetheless could be of high relevancy when studying the CFs and RS mechanism on a determined dielectric.

Studies on MIM devices showing both CW and CCW RS under certain conditions can be found in the literature. Changes in the switching polarity by changing the polarity of the forming process in $TiN/TiO_2/TiN$ films [15] or exchanging the bottom and top metal electrodes in $Pt/TiO_2/TiN$ stacks [16] were reported. In the former study, the authors attributed the difference in switching polarity to the drift of oxygen vacancies in the electroforming process. Both studies concluded that the breaking of the filament was induced at and by the interface between TiN and TiO_2 acting as a diffusion barrier for oxygen ions while TiN acts as an oxygen reservoir, if partially oxidized. Thus, the change in switching polarity in the latter study was due to the exchange of Pt and TiN as bottom or top electrodes.

A change in RS polarity due to the increase of the current compliance in the electroforming process in $Pt/TiO_2/Pt$ devices has been reported [17]. Bae et al. [18] reported that swapping the position of oxygen-rich TiO_x and oxygen-deficient TiO_y layers in $Pt/TiO_x/TiO_y/Pt$ devices can lead to CW and CCW RS, respectively. A more recent study on $Pt/TiO_2/TiON/TiN$ showed that an irreversible change from CCW RS to CW RS occurred by increasing RESET voltages [19]. However, in all these studies, CCW RS resistance states and switching (SET and RESET) voltages did not match those of the CW RS. Similar results have been observed in other materials such as Sr_2TiO_3 [20], in which different electroforming polarities led to different I-V hysteretic curves, either CW or CCW, and Sr_2TiO_4 [21], that showed co-existent and reversible CW and CCW RS behavior due to defect distribution.

Regarding the switching polarity dependence on film thickness, the previous research on that topic is also limited. Zhu et al. [22] have observed that NiO_x films showed different RS switching polarities. This was attributed to the formation of a metallic filament (ECM) for a 20 nm-thick film, and to the electron hopping through oxygen vacancies (VCM) for a 60 nm-thick sample. It has been demonstrated that WO_x films show filamentary RS characteristics below a certain threshold thickness, changing the resistive switching polarity [23,24]. Switching polarity has also been studied in $TiN/HfO_2/TiN$ devices [25] where both CW and CCW RS were seen to coexist due to the interlayers between TiN and HfO_2. These interlayers, responsible for the breaking of the CF, were formed near the bottom and top electrodes, as both of them were composed of TiN, which acts as an oxygen reservoir. Brivio et al. [26] reported that CW and CCW RS coexisted in $Pt/HfO_2/TiN$ junctions, and an in-depth study carried out by Petzold et al. [27] on $Pt/HfO_2/TiN$ structures determined that, in certain cases, it is possible to control the polarity of the BRS by choosing an appropriate voltage regime.

Understanding filament formation and behavior is essential to shed light on the underlying physics of the resistive switching effect. The present work shows a phenomenon not previously reported in the literature: resistive switching polarity change because of dielectric thickness without clear variation in the voltage regime, and with no relation with forming voltage or current compliance polarity in $TiN/Ti/HfO_2/Pt$ MIM devices. The goal was to examine samples grown to two functional thicknesses which are sufficiently low, close enough to each other, but clearly separable and distinguishable considering the measurement error ranges stated in the next section.

2. Materials and Methods

The TiN/Ti/HfO_2/Pt devices have a cross-point configuration as shown in Figure 1. They were fabricated on Si wafers covered with a thermally grown 200 nm SiO_2 layer. First, the bottom electrode was deposited and patterned by lift-off. This electrode consisted of a stack of 100 nm-thick Pt layers on a 5 nm Cr adhesion layer. Then, X-ray amorphous HfO_2 layers were grown by Atomic Layer Deposition (ALD) in a Picosun ^{TM} R-200 Advanced ALD reactor, using Tetrakis(ethylmethylamido)hafnium(IV) (TEMAH) as the hafnium precursor evaporated at 100 °C, and oxygen plasma as the oxygen source. Reactions were carried out at 200 °C, whereby one ALD cycle consisted in four sequential pulses: TEMAH pulse (0.3 s)—N_2 purge (8 s)—O_2 plasma pulse (15 s)—N_2 purge (8 s). The layers were grown to a thickness of 8 nm on one wafer and 13 nm on another one. The film thicknesses were measured with a GES5E spectroscopic ellipsometer (Semilab Sopra, Budapest, Hungary). The spectra were modeled using the Cauchy model in the range of 1.2767-5.00 eV by WinElli software. The uncertainty of the thickness determination, together with possible deviations in the thickness due to the growth profile, remains within 10% of the calculated value. The ellipsometry also revealed the refractive index values of 1.5 and 1.7 (at 633 nm) for 8 and 13 nm thick films, respectively, indicating that the thicker films have a higher density.

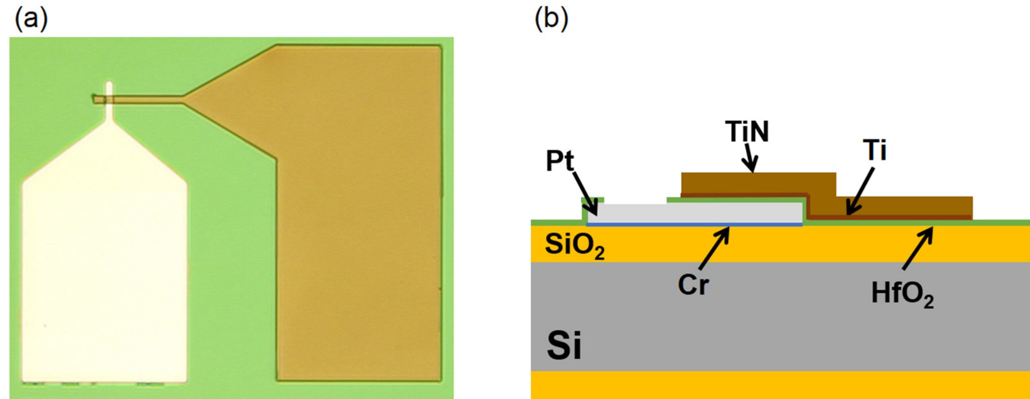

Figure 1. (**a**) Layout of the cross-point configuration. (**b**) Cross-section of the device.

After HfO_2 deposition, the top electrode consisting of 200 nm TiN on 10 nm Ti, was deposited by magnetron sputtering and patterned by photolithography and lift-off. Finally, the contact area to the bottom Pt electrode was defined by photolithography and dry etching of the HfO_2 layer. The resulting structures were square-shaped cells of 5×5 μm^2 area.

Resistive switching measurements were carried out by means of a Keithley 4200-SCS semiconductor parameter analyzer (Keysight Technologies, Cleveland, OH, USA) and a probe station. DC voltage was applied to the top electrode, while the bottom electrode was grounded. Current–voltage (I-V) measurements were made in order to characterize the electrical behavior of the devices by applying voltage sweeps.

3. Results

All the samples exhibited excellent resistive switching characteristics, with good repeatability and stability of the resistance states (Figure 2). SET transition occurred approximately at 0.8 V, while RESET took place at voltages higher than 1.5 V. The functional window between low and high resistance states (LRS and HRS) was of more than two orders of magnitude (at 0.1 V) for all the samples.

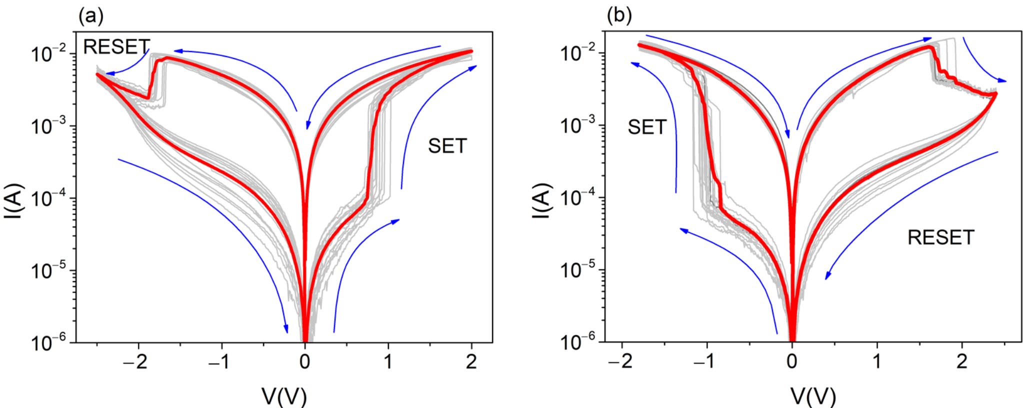

Figure 2. Current-Voltage curves of a TiN/Ti/HfO_2/Pt sample with a HfO_2 thickness of (**a**) 8 nm and (**b**) 13 nm. The red curve represents an average of the 50 I-V loop shown in grey.

When comparing the I-V curves of samples with an 8 nm thick HfO_2 layer (Figure 2a) with those of the thicker samples with a 13 nm thick HfO_2 layer (Figure 2b), it is seen that, although both devices presented similar resistive switching behavior in terms of the functional window between states and switching voltages, the polarity of the RS behavior was inverted between the 8 nm and 13 nm thick films. While the 8 nm thick film presents CCW RS, the 13 nm thick film shows CW RS. Although the polarity of the BRS is reversed, it can be seen that the I-V curves of both samples remain very similar, contrary to previous results in the literature reporting both CW and CCW RS [17–21,26].

The electroforming process was carried out using a current compliance of 1 µA, for both thickness, but at different polarities (Figure 3). In the case of the 8 nm film, the process occurred at a positive bias (3–4 V) whereas for the 13 nm case it took place at negative voltages (−8 V). The different polarities for the forming events were not searched for, rather the applied one was the polarity at which the dielectric layers in the different samples did not tend to break down irreversibly.

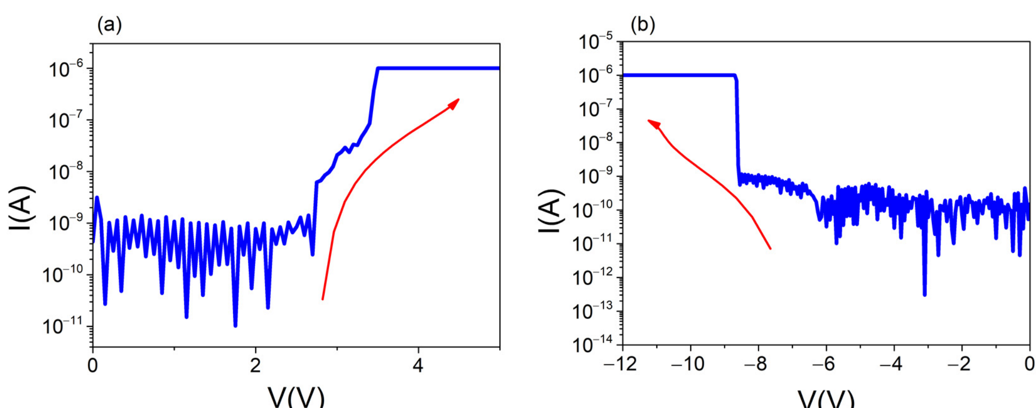

Figure 3. Electroforming process of a TiN/Ti/HfO_2/Pt sample with a HfO_2 thickness of (**a**) 8 nm and (**b**) 13 nm.

However, to rule out any experimenter bias, a positive forming process was applied to the 13 nm thick film (6.5 V), and a negative forming voltage to the 8 nm thick sample (−3 V). The results, depicted in Figures 4 and 5, showed that, indeed, the resistive switching polarity of the samples did not depend on the forming process, albeit the performance and the number of samples showing RS behavior improved with the adequate forming polarity. It was particularly interesting to observe the anomalous peak presented by the 13 nm thick HfO_2 sample after positive electroforming and a negative RESET process, which hints at

the underlying physics behind the resistive switching reported in this work, that will be discussed in Section 4.

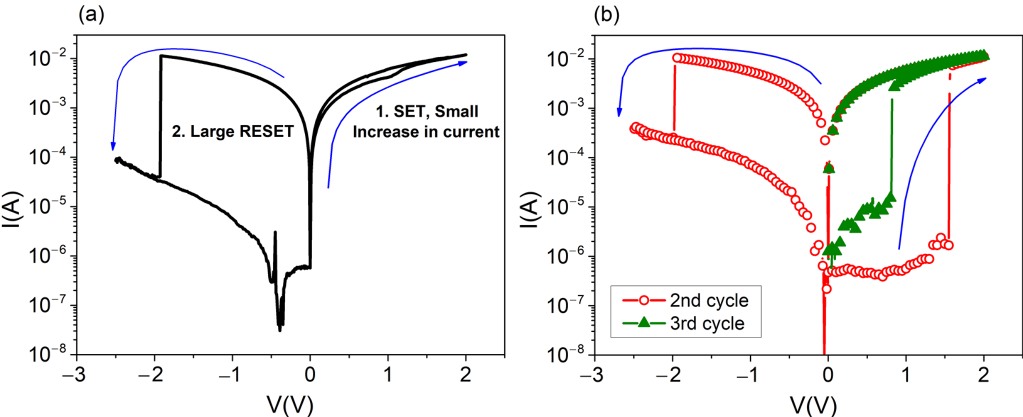

Figure 4. Resistive switching behaviour of the 8 nm film after a negative electroforming process. (**a**) 1st cycle after the electroforming. Positive voltage is applied first to initiate the RESET event and to invert the polarity. However, it does not occur (step 1), rather, a RESET can be seen when negative voltage is applied (step 2). (**b**) Two subsequent cycles, the sample still demonstrates CCW RS.

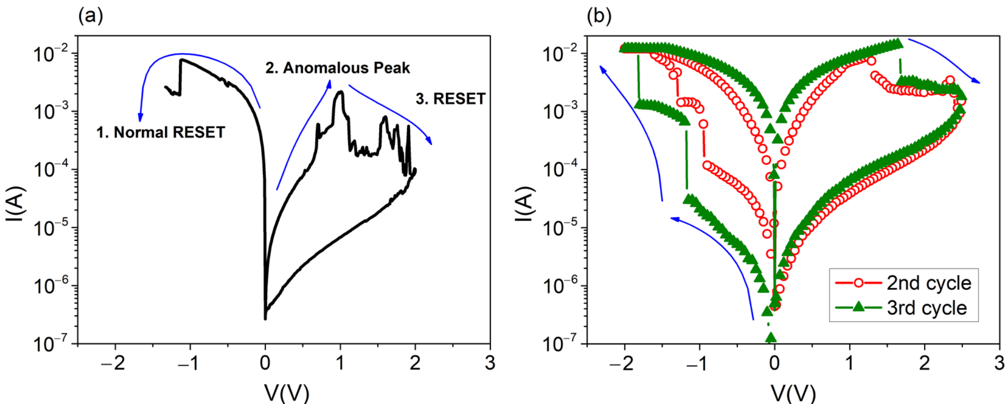

Figure 5. Resistive switching behaviour of the 13 nm film after a positive electroforming process. (**a**) 1st cycle after the electroforming. A negative voltage was applied to trigger the RESET event and confirm that the polarity had inverted (step 1). However, the device presented an anomalous peak resembling a failed SET event (step 2) after which a RESET occurs (step 3). (**b**) Two subsequent cycles, the sample still demonstrates CW RS.

4. Discussion

The CCW RS response of the thinner sample can be explained by the vacancy-rich zone in the HfO_2 layer generated due to Ti acting as an oxygen scavenger. One can propose that the filament is weak near the Pt electrode, where the iterative breaking and forming of the CF occurs. This has been studied by Goux et al. [28–30] and Giovinazzo et al. [31] in Pt/HfO_2/TiN and TiN/Ti/HfO_2/Pt devices, respectively. Both studies concluded that the CF formed between the metal electrodes is weakened near the Pt. As this metal is chemically inert, it does not form oxides and thus, no oxygen vacancy-rich zone is generated near the interface [28–33]. Meanwhile, both TiN and Ti are good oxygen reservoirs, which generate vacancy-rich zones in the hafnium oxide near the HfO_2/Ti or HfO_2/TiN interface [14,28,29,34]. More specifically, Ti capping is known to improve resistive switching properties due to its oxygen scavenging characteristics, the oxygen atoms move from the HfO_2 into the Ti layer, leaving oxygen vacancies behind and forming a TiO_x layer at the HfO_2/Ti interfaces [35–37], as depicted in Figure 6a.

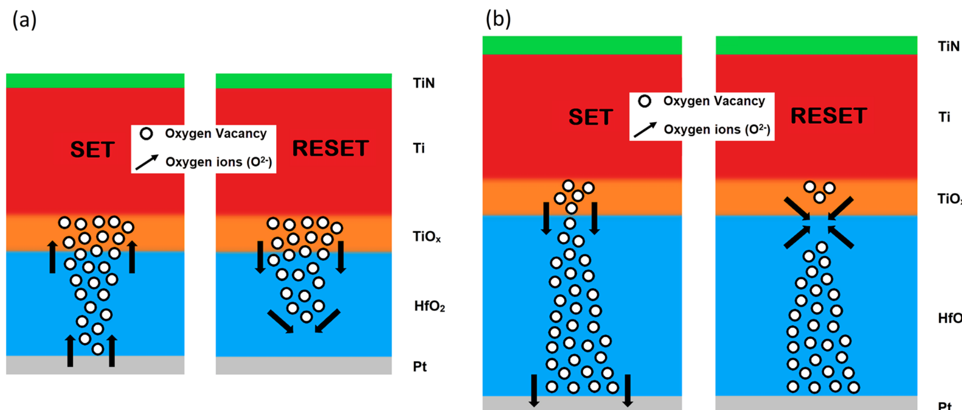

Figure 6. Proposed resistive switching mechanism for the (**a**) 8 nm and (**b**) 13 nm thick HfO_2 samples.

In the case of the 13 nm thick HfO_2 sample, the physical explanation, resistive switching mechanism and relevancy of dielectric thickness is not so simple to discuss, as it has been observed and discussed much less frequently in the literature. Because of this, we looked thoroughly into precedent research on this matter, in order to clarify the physics behind the polarity switch. As stated in several previously mentioned RRAM-related works discussing different BRS polarities [16,18,25,26,28–31], it is believed that the interface at which the filament disruption occurs determines if the BRS is CW or CCW. Thus, a tentative explanation would be that the different switching polarity can be attributed to a CF weaker near the Ti layer and thus, its disruption at the Ti/HfO_2 interface (Figure 6b), i.e., contrary to the previous case.

This explanation has been previously reported by Brivio et al. [26] in a study about CW and CCW RS coexisting (at different voltage regimes) on $Pt/HfO_2/TiN$ MIM stacks, which had the same metal electrodes as the ones presented by our devices. In this study, a competition between tendencies of CF dissolution at the different interfaces led to coexisting CW and CCW switching operations in the same 5.5 nm thick HfO_2 $Pt/HfO_2/TiN$ structure. Here, it is stated that current overshoot due to parasitic capacitances discharge or inefficient current limitation [38–40] led to further ion migration after the electroforming process, rearranging the CF with its thicker part near the Pt electrode. Due to the similarities with the structure studied in this article, this could be a plausible explanation for the RS mechanism proposed in Figure 6b for the 13 nm thick HfO_2 film. Moreover, parasitic capacitance discharge has also been theorized to cause current overshoot in CuO_x devices [41]. When the SET process occurs, the parasitic capacitance is charged to V_{SET}, and thus, when the device switches from HRS to LRS, the charges are stored in the capacitance discharge, leading to current overshoot, which could explain the re-arrangement of the CF as stated by Brivio et al.

Furthermore, the anomalous RESET peak observed in the present study upon the positive forming process in this film (Figure 5a) was also observed by Brivio et al. [26] when changing the switching operation. We also believe that this anomalous peak could indicate the competition between two filaments in the 13 nm thick HfO_2 sample, one thicker near the Ti layer, and one also thicker near the Pt electrode that ends up prevailing. In fact, in the case of the 13 nm thick HfO_2 device, the Ti layer is not thicker than the HfO_2 layer (which is the case for the thinner sample). This could prevent the formation of a large enough oxygen vacancy-rich zone at the HfO_2/Ti interface. This has proven to be the case in a study conducted by Hardtdegen et al. in $Pt/HfO_2/Ti/Pt$ films [42] where, in fact, because of the Ti cap being thinner than the thickness of the HfO_2 layer, a change in the BRS polarity occurred, partially attributed to full Ti cap oxidation. The RS mechanisms proposed could be further favored by a high negative voltage value needed to carry the forming process (although as it was earlier discussed, negative forming resulted in better performance and overall higher number of functional devices but was not mandatory). In addition, it must be mentioned that, although chemically inert, Pt is often used as a catalyst to adsorb O_2

on its surface [43,44], this could help the previously mentioned mechanisms by generating oxygen vacancies near the Pt surface.

Although it is clear that the HfO_2 thickness and/or the Ti/HfO_2 thickness ratio of the devices is the reason behind the effect that produces the polarity change of the BRS, it should be noted that no clear dependence between dielectric thickness and polarity can be determined. Nonetheless, as precedent research on redox-based RRAM presenting VCM suggests, no clear dependence of RS parameters such as LRS, HRS, LRS/HRS ratio or switching voltages with film thickness should be expected [45–47]. Only forming voltage has shown a dependence with thickness [48,49], with some devices even turning forming-free if the dielectric is sufficiently thin [50,51]. Forming voltage, however, is an RS parameter clearly differentiated from the rest by the fact that the electroforming process is made when the sample is in a pristine state, and thus, there are no conductive filaments, making the thickness dependence unsurprising.

Therefore, it is unlikely that resistive switching polarity may present a linear or clear dependence with thickness. Rather, as it is stated by previous studies on resistive switching media, certain RS characteristics may appear at optimal compositions or stoichiometries [45,47,52,53].

5. Conclusions

TiN/Ti/HfO_2/Pt devices with 8 nm and 13 nm thick HfO_2 layers demonstrated resistive switching characteristics. A change in the RS polarity of the samples with the HfO_2 layer thickness was observed. While the thinner sample demonstrated counter-clockwise RS behavior, the current-voltage curves recorded from the 13 nm thick HfO_2 film were described by clockwise behavior. However, the switching voltages remained similar for both samples/polarities, and no relation with forming voltage/current compliance polarity could be observed, being this experimental result a new finding as compared to previously published results in the literature. A thorough investigation of foregoing reported cases and studies on reversible and irreversible CW—CCW RS changes leads to the hypothesis that polarity change is due to filament disruption occurring at different interfaces. The thinner sample presents a Ti cap layer thicker than the HfO_2 which ensures its role as an oxygen reservoir, creating an oxygen vacancy-rich zone in the HfO_2 near the interface. Meanwhile, the filament is weaker near the Pt electrode due to its inert chemical nature. The opposite occurs for the thicker sample. It is believed that, in this case, current overshooting due to parasitic capacitances discharge, in addition to a relatively thinner Ti cap when compared to the HfO_2 layer, led to the formation of an oxygen vacancy-rich zone near the Pt electrode. Thus, the filament would present its weaker/thinner part near the Ti layer, changing the switching polarity.

Author Contributions: Conceptualization, G.V.; methodology, G.V., H.G., H.C., S.D.; investigation, G.V., K.K. (Kristjan Kalam), M.Z., A.T. (Aivar Tarre); resources, M.B.G., A.T. (Aile Tamm), K.K. (Kaupo Kukli), F.C., H.C., S.D.; writing—original draft, G.V.; writing—review and editing, H.G., M.B.G., K.K. (Kaupo Kukli), F.C., J.J., H.C., S.D.; funding acquisition, A.T. (Aile Tamm), K.K. (Kaupo Kukli), F.C., H.C. and S.D. All authors have read and agreed to the published version of the manuscript.

Funding: This research was funded by the Spanish Ministry of Science, Innovation and Universities and the FEDER program through projects TEC2017-84321-C4-1-R, and TEC2017-84321-C4-2-R. The study was partially supported by European Regional Development Fund project "Emerging orders in quantum and nanomaterials" (TK134), and Estonian Research Agency (PRG753).

Conflicts of Interest: The authors declare no conflict of interest.

References

1. Xu, N.; Gao, B.; Liu, L.; Sun, B.; Liu, X.; Han, R.; Kang, J.; Yu, B. A Unified Physical Model of Switching Behavior in Oxide-Based RRAM. In Proceedings of the 2008 Symposium on VLSI Technology, Honolulu, HI, USA, 17–19 June 2008; pp. 100–101.
2. Huang, P.; Liu, X.Y.; Li, W.H.; Deng, Y.X.; Chen, B.; Lu, Y.; Gao, B.; Zeng, L.; Wei, K.L.; Du, G.; et al. A Physical Based Analytic Model of RRAM Operation for Circuit Simulation. In Proceedings of the 2012 IEDM, San Francisco, CA, USA, 10–13 December 2012.
3. Lee, J.S.; Lee, S.; Noh, T.W. Resistive switching phenomena: A review of statistical physics approaches. *Appl. Phys. Rev.* **2015**, *2*, 031303. [CrossRef]
4. Wouters, D.J.; Waser, R.; Wuttig, M. Phase-Change and Redox-Based Resistive Switching Memories. *Proc. IEEE* **2015**, *103*, 1274–1288. [CrossRef]
5. Lanza, M. A Review on Resistive Switching in High-k Dielectrics: A Nanoscale Point of View Using Conductive Atomic Force Microscope. *Materials* **2014**, *7*, 2155–2182. [CrossRef]
6. Ye, C.; Wu, J.; He, G.; Zhang, J.; Deng, T.; He, P.; Wang, H. Physical Mechanism and Performance Factors of Metal Oxide Based Resistive Switching Memory: A Review. *J. Mater. Sci. Technol.* **2016**, *32*, 1–11. [CrossRef]
7. Cavallini, M.; Hemmatian, Z.; Riminucci, A.; Prezioso, M.; Morandi, V.; Murgia, M. Regenerable Resistive Switching in Silicon Oxide Based Nanojunctions. *Adv. Mater.* **2012**, *24*, 1197–1201. [CrossRef] [PubMed]
8. Chen, W.; Lu, W.; Long, B.; Li, Y.; Gilmer, D.; Bersuker, G.; Bhunia, S.; Jha, R. Switching characteristics of W/Zr/HfO2/TiN ReRAM devices for multi-level cell non-volatile memory applications. *Semicond. Sci. Technol.* **2015**, *30*, 075002. [CrossRef]
9. Dueñas, S.; Castán, H.; García, H.; Miranda, E.; Gonzalez, M.; Campabadal, F. Study of the admittance hysteresis cycles in TiN/Ti/HfO2/W-based RRAM devices. *Microelectron. Eng.* **2017**, *178*, 30–33. [CrossRef]
10. Rodriguez-Fernandez, A.; Cagli, C.; Perniola, L.; Miranda, E.; Suñé, J. Characterization of HfO2-based devices with indication of second order memristor effects. *Microelectron. Eng.* **2018**, *195*, 101–106. [CrossRef]
11. Niinistö, J.; Kukli, K.; Heikkilä, M.; Ritala, M.; Leskelä, M. Atomic Layer Deposition of High-kOxides of the Group 4 Metals for Memory Applications. *Adv. Eng. Mater.* **2009**, *11*, 223–234. [CrossRef]
12. Ossorio, O.G.; Poblador, S.; Vinuesa, G.; Duenas, S.; Castan, H.; Maestro-Izquierdo, M.; Bargallo, M.G.; Campabadal, F. Single and Complex Devices on Three Topological Configurations of HfO2 Based RRAM. In Proceedings of the 2020 IEEE LAEDC, San José, Costa Rica, 25–28 February 2020; pp. 1–4.
13. Makarov, A.; Sverdlov, V.; Selberherr, S. Stochastic model of the resistive switching mechanism in bipolar resistive random-access memory: Monte Carlo simulations. *J. Vac. Sci. Technol. B Nanotechnol. Microelectron. Mater. Process. Meas. Phenom.* **2011**, *29*, 01AD03. [CrossRef]
14. Feng, W.; Shima, H.; Ohmori, K.; Akinaga, H. Investigation of switching mechanism in HfOx-ReRAM under low power and conventional operation modes. *Sci. Rep.* **2016**, *6*, 39510. [CrossRef]
15. Kwak, J.S.; Do, Y.H.; Bae, Y.C.; Im, H.S.; Yoo, J.H.; Sung, M.G.; Hwang, Y.T.; Hong, J.P. Roles of interfacial TiOxN1−x layer and TiN electrode on bipolar resistive switching in TiN/TiO2/TiN frameworks. *Appl. Phys. Lett.* **2010**, *96*, 223502. [CrossRef]
16. Do, Y.H.; Kwak, J.S.; Bae, Y.C.; Lee, J.H.; Kim, Y.; Im, H.; Hong, J.P. TiN electrode-induced bipolar resistive switching of TiO2 thin films. *Curr. Appl. Phys.* **2010**, *10*, e71–e74. [CrossRef]
17. Kim, K.M.; Kim, G.H.; Song, S.J.; Seok, J.Y.; Lee, M.H.; Yoon, J.H.; Hwang, C.S. Electrically configurable electroforming and bipolar resistive switching in Pt/TiO2/Pt structures. *Nanotechnology* **2010**, *21*, 305203. [CrossRef] [PubMed]
18. Bae, Y.C.; Lee, A.R.; Bin Lee, J.; Koo, J.H.; Kwon, K.C.; Park, J.G.; Im, H.S.; Hong, J.P. Oxygen Ion Drift-Induced Complementary Resistive Switching in Homo TiOx/TiOy/TiOxand Hetero TiOx/TiON/TiOxTriple Multilayer Frameworks. *Adv. Funct. Mater.* **2011**, *22*, 709–716. [CrossRef]
19. Biju, K.P. Resistive switching characteristics of thermally oxidized TiN thin films. *AIP Conf. Proc.* **2018**, *1942*, 060023. [CrossRef]
20. Yan, X.B.; Xia, Y.D.; Xu, H.N.; Gao, X.; Li, H.T.; Li, R.; Yin, J.; Liu, Z.G. Effects of the electroforming polarity on bipolar resistive switching characteristics of SrTiO3−δ films. *Appl. Phys. Lett.* **2010**, *97*, 112101. [CrossRef]
21. Shibuya, K.; Dittmann, R.; Mi, S.; Waser, R. Impact of Defect Distribution on Resistive Switching Characteristics of Sr2TiO4Thin Films. *Adv. Mater.* **2010**, *22*, 411–414. [CrossRef]
22. Zhu, H.X.; Huo, J.Q.; Qiu, X.Y.; Zhang, Y.Y.; Wang, R.X.; Chen, Y.; Wong, C.M.; Yau, H.M.; Dai, J.Y. Thickness-Dependent Bipolar Resistive Switching Behaviors of NiO_x Films. *Mater. Sci. Forum* **2016**, *847*, 131–136. [CrossRef]
23. Biju, K.P.; Liu, X.; Siddik, M.; Kim, S.; Shin, J.; Kim, I.; Ignatiev, A.; Hwang, H. Resistive switching characteristics and mechanism of thermally grown WOx thin films. *J. Appl. Phys.* **2011**, *110*, 64505. [CrossRef]
24. Biju, K.P.; Liu, X.; Kim, S.; Jung, S.; Park, J.; Hwang, H. Coexistence of filamentary and homogeneous resistive switching in graded WO x thin films. *Phys. Status Solidi Rapid Res. Lett.* **2011**, *5*, 89–91. [CrossRef]
25. Zhang, H.Z.; Ang, D.S.; Gu, C.J.; Yew, K.S.; Wang, X.P.; Lo, G.Q. Role of interfacial layer on complementary resistive switching in the TiN/HfOx/TiN resistive memory device. *Appl. Phys. Lett.* **2014**, *105*, 222106. [CrossRef]
26. Brivio, S.; Frascaroli, J.; Spiga, S. Role of metal-oxide interfaces in the multiple resistance switching regimes of Pt/HfO2/TiN devices. *Appl. Phys. Lett.* **2015**, *107*, 023504. [CrossRef]
27. Petzold, S.; Miranda, E.; Sharath, S.U.; Muñoz-Gorriz, J.; Vogel, T.; Piros, E.; Kaiser, N.; Eilhardt, R.; Zintler, A.; Molina-Luna, L.; et al. Analysis and simulation of the multiple resistive switching modes occurring in HfOx-based resistive random-access memories using memdiodes. *J. Appl. Phys.* **2019**, *125*, 234503. [CrossRef]

28. Goux, L.; Chen, Y.-Y.; Pantisano, L.; Wang, X.-P.; Groeseneken, G.; Jurczak, M.; Wouters, D.J. On the Gradual Unipolar and Bipolar Resistive Switching of TiN\HfO2\Pt Memory Systems. *Electrochem. Solid State Lett.* **2010**, *13*, G54–G56. [CrossRef]
29. Goux, L.; Wang, X.P.; Chen, Y.Y.; Pantisano, L.; Jossart, N.; Govoreanu, B.; Kittl, J.A.; Jurczak, M.; Altimime, L.; Wouters, D.J. Roles and Effects of TiN and Pt Electrodes in Resistive-Switching HfO2 Systems. *Electrochem. Solid State Lett.* **2011**, *14*, H244–H246. [CrossRef]
30. Goux, L.; Czarnecki, P.; Chen, Y.Y.; Pantisano, L.; Wang, X.P.; Degraeve, R.; Govoreanu, B.; Jurczak, M.; Wouters, D.J.; Altimime, L. Evidence of oxygen-mediated resistive-switching mechanism in TiN\HfO2\Pt cells. *Appl. Phys. Lett.* **2010**, *97*, 243509. [CrossRef]
31. Giovinazzo, C.; Sandrini, J.; Shahrabi, E.; Celik, O.T.; Leblebici, Y.; Ricciardi, C. Analog Control of Retainable Resistance Multistates in HfO2 Resistive-Switching Random Access Memories (ReRAMs). *ACS Appl. Electron. Mater.* **2019**, *1*, 900–909. [CrossRef]
32. Wang, Z.; Jiang, H.; Jang, M.H.; Lin, P.; Ribbe, A.; Xia, Q.; Yang, J.J. Electrochemical metallization switching with a platinum group metal in different oxides. *Nanoscale* **2016**, *8*, 14023–14030. [CrossRef]
33. Raffone, F.; Cicero, G. Does platinum play a role in the resistance switching of ZnO nanowire-based devices? *Solid State Ion.* **2017**, *299*, 93–95. [CrossRef]
34. Lee, H.Y.; Chen, Y.S.; Wu, T.Y.; Chen, F.; Wang, C.C.; Tzeng, P.J.; Tsai, M.-J.; Lien, C.-H. Low-Power and Nanosecond Switching in Robust Hafnium Oxide Resistive Memory with a Thin Ti Cap. *IEEE Electron Device Lett.* **2009**, *31*, 44–46. [CrossRef]
35. Fang, Z.; Wang, X.P.; Sohn, J.; Bin Weng, B.; Zhang, Z.P.; Chen, Z.X.; Tang, Y.Z.; Lo, G.-Q.; Provine, J.; Wong, S.S.; et al. The Role of Ti Capping Layer in HfOx-Based RRAM Devices. *IEEE Electron Device Lett.* **2014**, *35*, 912–914. [CrossRef]
36. Gao, B.; Yu, S.; Xu, N.; Liu, L.; Sun, B.; Liu, X.; Han, R.; Kang, J.; Yu, B.; Wang, Y. Oxide-Based RRAM Switching Mechanism: A New Ion-Transport-Recombination Model. In Proceedings of the IEDM, San Francisco, CA, USA, 15–17 December 2008; pp. 1–4.
37. Dirkmann, S.; Kaiser, J.; Wenger, C.; Mussenbrock, T. Filament Growth and Resistive Switching in Hafnium Oxide Memristive Devices. *ACS Appl. Mater. Interfaces* **2018**, *10*, 14857–14868. [CrossRef] [PubMed]
38. Kinoshita, K.; Tsunoda, K.; Sato, Y.; Noshiro, H.; Yagaki, S.; Aoki, M.; Sugiyama, Y. Reduction in the reset current in a resistive random-access memory consisting of NiOx brought about by reducing a parasitic capacitance. *Appl. Phys. Lett.* **2008**, *93*, 033506. [CrossRef]
39. Gilmer, D.C.; Bersuker, G.; Park, H.-Y.; Park, C.; Butcher, B.; Wang, W.; Kirsch, P.D.; Jammy, R. Effects of RRAM Stack Configuration on Forming Voltage and Current Overshoot. In Proceedings of the 3rd IEEE IMW, Monterey, CA, USA, 22–25 May 2011.
40. Bersuker, G.; Gilmer, D.C.; Veksler, D.; Kirsch, P.; Vandelli, L.; Padovani, A.; Larcher, L.; McKenna, K.; Shluger, A.; Iglesias, V.; et al. Metal oxide resistive memory switching mechanism based on conductive filament properties. *J. Appl. Phys.* **2011**, *110*, 124518. [CrossRef]
41. Wan, H.J.; Zhou, P.; Ye, L.; Lin, Y.Y.; Tang, T.A.; Wu, H.M.; Chi, M.H. In Situ Observation of Compliance-Current Overshoot and Its Effect on Resistive Switching. *IEEE Electron. Device Lett.* **2010**, *31*, 246–248. [CrossRef]
42. Hardtdegen, A.; Zhang, H.; Hoffmann-Eifert, S. Tuning the Performance of Pt/HfO2/Ti/Pt ReRAM Devices Obtained from Plasma-Enhanced Atomic Layer Deposition for HfO2 Thin Films. *ECS Trans.* **2016**, *75*, 177–184. [CrossRef]
43. Cao, K.; van Lent, R.; Kleyn, A.W.; Kurahashi, M.; Juurlink, L.B.F. Steps on Pt stereodynamically filter sticking of O2. *Proc. Natl. Acad. Sci. USA* **2019**, *116*, 13862–13866. [CrossRef]
44. Gutiérrez-González, A.; Beck, R.D. Unraveling the complexity of oxygen reactions on Pt surfaces. *Proc. Natl. Acad. Sci. USA* **2019**, *116*, 13727–13728. [CrossRef]
45. Nakajima, R.; Azuma, A.; Yoshida, H.; Shimizu, T.; Ito, T.; Shingubara, S. Hf layer thickness dependence of resistive switching characteristics of Ti/Hf/HfO2/Au resistive random access memory device. *Jpn. J. Appl. Phys.* **2018**, *57*, 06HD06. [CrossRef]
46. Hsieh, C.-C.; Roy, A.; Rai, A.; Chang, Y.-F.; Banerjee, S.K. Characteristics and mechanism study of cerium oxide based random access memories. *Appl. Phys. Lett.* **2015**, *106*, 173108. [CrossRef]
47. Hong, S.K.; Kim, J.E.; Kim, S.O.; Choi, S.-Y.; Cho, B.J. Flexible Resistive Switching Memory Device Based on Graphene Oxide. *IEEE Electron. Device Lett.* **2010**, *31*, 1005–1007. [CrossRef]
48. Govoreanu, B.; Kar, G.; Chen, Y.-Y.; Paraschiv, V.; Kubicek, S.; Fantini, A.; Radu, I.; Goux, L.; Clima, S.; Degraeve, R.; et al. 1010 nm^2 Hf/HfOx Crossbar Resistive RAM with Excellent Performance, Reliability and Low-Energy Operation. In Proceedings of the International Electron Devices Meeting, Washington, DC, USA, 5–7 December 2011.
49. Lee, H.Y.; Chen, P.S.; Wu, T.Y.; Chen, Y.S.; Wang, C.C.; Tzeng, P.J.; Lin, C.H.; Chen, F.; Lien, C.H.; Tasi, M.J. Low Power and High-Speed Bipolar Switching with a Thin Reactive Ti Buffer Layer in Robust HfO2 Based RRAM. In Proceedings of the 2008 IEEE International Electron Devices Meeting, San Francisco, CA, USA, 14–17 December 2008.
50. Bruchhaus, R.; Hermes, C.; Waser, R. Memristive Switches with Two Switching Polarities in a Forming Free Device Structure. *MRS Proc.* **2011**, *1337*, 803. [CrossRef]
51. Jeong, D.S.; Choi, B.J.; Hwang, C.S. Electroforming Processes in Metal Oxide Resistive-Switching Cells. In *Resistive Switching*; Ielmini, D., Waser, R., Eds.; John Wiley & Sons, Ltd.: Hoboken, NJ, USA, 2016; pp. 289–316.
52. McKenna, K.P. Optimal stoichiometry for nucleation and growth of conductive filaments in HfOx. *Model. Simul. Mater. Sci. Eng.* **2014**, *22*, 025001. [CrossRef]
53. He, S.; Hao, A.; Qin, N.; Bao, D. Unipolar resistive switching properties of Pr-doped ZnO thin films. *Ceram. Int.* **2017**, *43*, S474–S480. [CrossRef]